Compressibility Divergence and Mott Endpoints

G. Kotliar* Sahana Murthy* and M.J. Rozenberg+
Serin Physics Laboratory, Rutgers University, 136 Frelinghuysen Road, Piscataway, New Jersey 08854, USA
+*Departamento de Física, FCEN, Universidad de Buenos Aires, Ciudad Universitaria Pab.I, (1428) Buenos Aires, Argentina.*
(February 1, 2008)

In the context of the dynamical mean field theory of the Hubbard model, we study the behavior of the compressibility near the density driven Mott transition at finite temperatures. We demonstrate this divergence using dynamical mean field theory and Quantum Monte Carlo simulations in the one band and the two band Hubbard model. We supplement this result with considerations based on the Landau theory framework, and discuss the relevance of our results to the α-γ endpoint in Cerium.

PACS Numbers: 71.30.+h, 71.10.Fd, 71.27.+a

The Mott transition, namely the metal-insulator transition (MIT) driven by electron-electron interactions [1], is a fascinating phenomenon realized experimentally in many compounds such as V_2O_3 and $Ni(Se,S)_2$ [2]. The Mott transition concept is also relevant to elements in the lanthanide and actinide series [3]. Viewed from a broader perspective, the Mott transition problem forces us to develop tools to describe materials where the electron is not fully described by either a real space picture or a momentum space picture, and continues to spur advances in many body and electronic structure methods.

On the theory side, the Hubbard model is the simplest Hamiltonian that captures some of the essential physics of the transition. It has been intensively studied in one dimension, but in this limit no finite temperature phase transitions can take place. In recent years, theoretical progress has been made in the understanding of the Mott-Hubbard transition using the dynamical mean-field theory (DMFT) [4]. In this framework, Mott transition points can be viewed as bifurcation points of a functional [5,6] of the local Greens function G, or of its associated variable, the Weiss field which describes the local environment of a correlated site.

The case of the correlation strength (U) driven MIT at half filling, is now well understood. At temperature $T = 0$ there are two bifurcation points, one denoted by $U_{c1}(T = 0)$ where the insulating solution disappears, and the other denoted by $U_{c2}(T = 0)$ where the metallic state disappears in a fashion reminiscent to the Brinkman Rice scenario [7]. It was found that in the U-T phase diagram of the frustrated Hubbard model there is a first-order MIT line [8,9] that ends in a finite temperature second-order critical point (T_{MIT}, U_{MIT}) which has the character of a regular Ising bifurcation with a rapid variation of the susceptibility connected to the double occupancy [10,11]. At higher temperatures the $U_{c2}(T)$ and $U_{c1}(T)$ lines become crossover lines, which have a well defined experimental significance discussed in [12].

The zero temperature aspects of the doping driven MIT were studied in [13]. It was shown that there are two solutions in an area bound by the curves μ_{c1}, where the insulating solution disappears, and μ_{c2}, where the metallic state disappears. The finite temperature aspects of the doping driven Mott transition have not been investigated so far. This is the subject of this paper. We will not consider the effects of long range order.

Our main interest is the behavior of the charge compressibility near the doping driven Mott transition in the paramagnetic phase at finite temperatures. Furukawa and Imada [14] pointed out that the compressibility diverges at the density driven Mott transition in 2-dimensions at $T = 0$. This behavior has been also observed on other models of correlated electron systems such as the t-J model indicating that this phenomenon is quite general [15]. Simple models of the Mott transition, such as the Gutzwiller approximation or the slave-boson approach predict a finite compressibility [16]. It is very important to understand the physical origin of this result, and to see if it is realized in the DMFT solution of the Hubbard model. The previously investigated bifurcation points within the DMFT, have either a finite charge compressibility, such as in the $T = 0$ density driven Mott transition, or a vanishing charge compressibility, as in the $T = 0$ correlation driven transition.

Our study of the neighborhood of the Mott transition endpoint is relevant to materials which have a finite temperature isostructural phase transition such as Cerium. This can be seen by generalizing the derivation of the Landau free energy of [11]. Near the transition, the free energy of more complicated models would have the same form as that studied in our paper.

We start with the m-band degenerate Hubbard model:

$$H - \mu N = -\frac{t}{\sqrt{z}} \sum_{\langle ij\rangle m\sigma} c^{\dagger}_{im\sigma} c_{jm\sigma} + \frac{U}{2} \sum_{i,m,m'\sigma} n_{im\sigma} n_{im'-\sigma} + \frac{U}{2} \sum_{i,m\neq m'\sigma} n_{im\sigma} n_{im'\sigma} - \mu \sum_{im\sigma} n_{im\sigma} \qquad (1)$$

The first term describes the hopping between nearest neighbors $\langle ij\rangle$ on a lattice with coordination number z. $m, m' = 1, 2$ are the band indices and $\sigma = \uparrow, \downarrow$ labels the

spin index. The parameter U is the energy cost associated with having a double occupancy on each site. t and U are assumed to be independent of the band indices and we concentrate on the paramagnetic phase. In the limit of infinite dimensions, $z \to \infty$, this model can be mapped onto a single-impurity Anderson model (SIAM) supplemented by a self-consistency condition [4]. The DMFT equation of the model reads

$$t^2 G_{m\sigma}(i\omega_n)[\Delta, \alpha] = \Delta(i\omega_n) \qquad (2)$$

where ω_n are the fermionic Matsubara frequencies, $G_{m\sigma}$ is the impurity Green's function and Δ is the hybridization function of the SIAM. Here, α denotes the control parameter such as temperature T, Coulomb repulsion U, chemical potential μ, etc. We adopt a semicircular density of states, $\rho(\epsilon) = (\frac{2}{\pi D})\sqrt{1-(\epsilon/D)^2}$ where the half-bandwidth $D = 2t = 1$ is our unit of energy.

We now propose a schematic phase diagram (Fig. 1) for the degenerate Hubbard model. The figure shows cross sections of the T-μ plane for various values of the interaction U. In the particle-hole symmetric case in the 1-band model the peaks have equal height. The shaded regions indicate coexistence between metallic and insulating solutions. The presence of a coexistence region and a first order phase transition in 2-band model was apparent in earlier Monte Carlo calculations [17]. This also follows from the general form of the Landau functional of this problem [5], which has the same form for the 1-band and and the multiband situations. The finite temperature and general chemical potential aspects of this problem had not been discussed before in the literature.

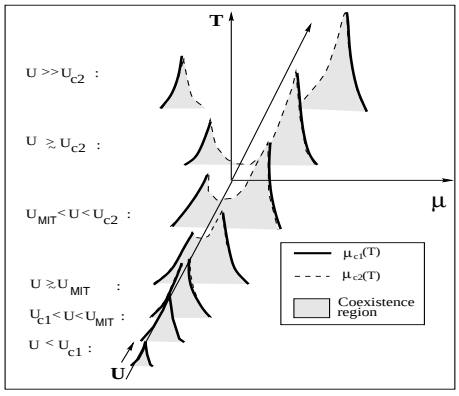

FIG. 1. Schematic phase diagram for the degenerate Hubbard model. The cross sections shown are on the T-μ plane for different values of U. μ_{c1} (the heavy line) and U_{c1} are the chemical potential and interaction respectively at which the insulating solution gets destroyed. μ_{c2} (the dotted line) and U_{c2} are the chemical potential and interaction at which the metallic solution gets destroyed. U_{MIT} is the value of the interaction at which the MIT endpoint takes place.

On solving the DMFT equation (2) iteratively using quantum Monte Carlo (QMC) methods, we find that at

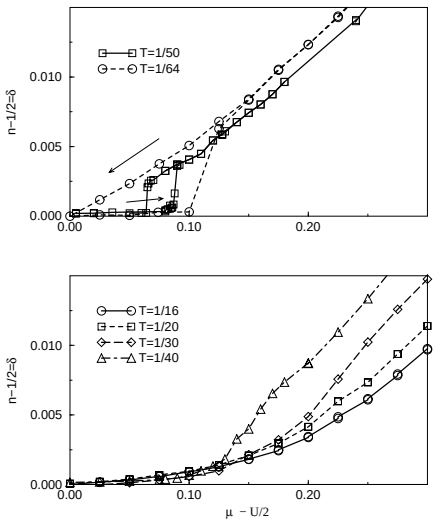

FIG. 2. Particle occupation $\delta = \langle n \rangle$-1/2 per spin as a function of the shifted chemical potential $\mu - U/2$ for different temperatures T. The lower panel shows QMC data obtained at $T = 1/40, 1/30, 1/20, 1/16$ (right to left) which are above $T_{\rm MIT}$. The upper panel shows similar data at temperatures $T = 1/64, 1/50$ which are below $T_{\rm MIT}$. The left arrow indicates that starting at high doping, a metallic solution can be followed down to half-filling. Also, starting from an insulating state at half-filling, one can follow the coexisting solution (right arrow) by increasing μ up to a sudden jump in δ.

integer filling, for smaller values of U ($< U_{c1}$ in Fig. 1) the solutions show metallic behavior while for large values of U ($> U_{c2}$ in Fig. 1) the solutions show insulating behavior. In Fig.2 we show the results for the doping (per spin) $\delta = \langle n \rangle - 1/2$ as a function of the chemical potential μ obtained from QMC calculations with $\Delta\tau = 0.5$ in the single band case. The interaction value $U = 2.46$ is inside the small region of coexisting solutions when the system is at half-filling [10]. In the lower panel we show the results at several temperatures above the critical temperature T_{MIT}. As the temperature is decreased the curves develop a sigmoidal shape, which is a hallmark of the approach to a second order critical point in Landau theory, as in the familiar Ising mean-field model.

The results for the total occupation number n as a function of μ in the 2-band model are shown in Fig.3. The QMC calculation was carried out at $\Delta\tau = 0.25$ and $U = 3.0$. At higher temperatures, only one solution is present, whereas on lowering the temperature to $T = 1/40$ both metallic and insulating solutions coexist.

To obtain coexisting solutions below T_{MIT} we first start at high doping in a metallic state as indicated by the left arrow in the upper panel of Fig.2. For this, we use a seed from low U ($< U_{c1}$ in Fig.1) and continuously evolve towards integer filling through the upper branch solution which always remains metallic with finite compressibility. We use a self-consistent solution as new seed for the successive calculations at smaller μ. On the other hand,

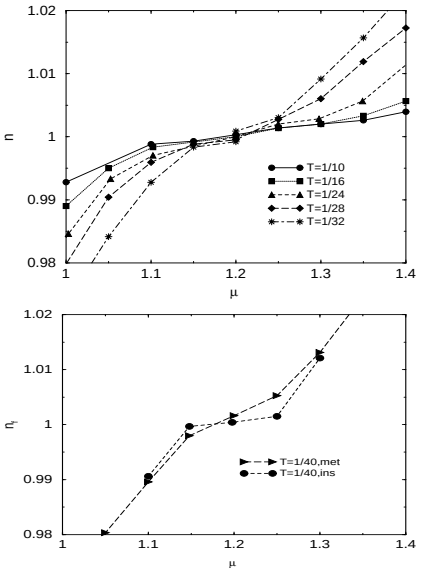

FIG. 3. Particle occupation n function of μ for different temperatures. in the 2-band model at U=3.0. In the upper panel, the temperatures are above the critical temperature while in the lower panel, we see coexistence at $T < T_{MIT}$.

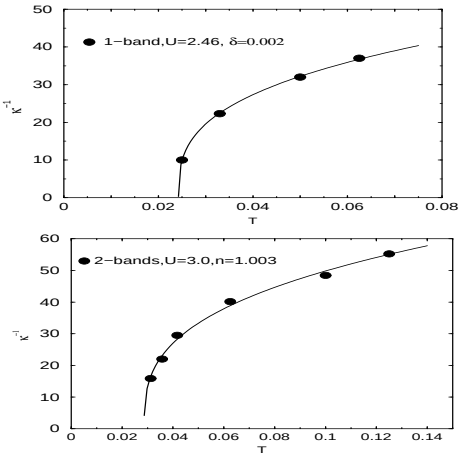

FIG. 4. The inverse compressibility κ^{-1}, obtained by the numerical differentiation of n with respect to μ, at a constant doping as a function of T. Top: 1-band model at $U = 2.46$ with doping $\delta = 0.002$. Bottom: 2-band model at $U = 3.0$ at $n = 1.003$. The solid lines are a guide to the eye.

a second solution is also present at half-filling in Fig.2 (or near $n = 1$ in Fig.3) corresponding to an insulting-like state, obtained by using a seed from large U ($> U_{c2}$ in Fig. 1). This state is essentially incompressible as n almost remains constant while increasing μ. This can be continuously followed as μ is increased until the eventual jump of n towards the unique solution present at the higher values of μ. This procedure successfully determined the location of the coexisting region [18].

Locating these parameters in the schematic phase diagram, we find that the data for the 1-band model below T_{MIT} in Fig. 2 corresponds to the region near the right peak at $U_{MIT} < U < U_{c2}$ in Fig. 1. As we move towards $\delta = 0$ in the metallic phase, we cross the coexistence region and reach the μ_{c2} line at $T = 1/50$. Upon lowering T to $1/64$ we can approach $\delta = 0$ without crossing the μ_{c2} line. In the 2-band model, it was found that at $T = 1/40$ the insulating solution disappears as we move away from $n = 1$ indicating the the μ_{c1} line has been crossed indicating that the data in Fig. 3 lies near the right peak at $U_{MIT} < U < U_{c2}$ in Fig. 1.

The region with two coexisting solutions has two different values of n for given T and μ. These two coexisting solutions have different free energies and the actual thermodynamic state of the system will be that of minimum energy. Therefore, a jump in the particle occupation is predicted at a first-order line. The actual determination of this line, thus implies a precise calculation of the free energy which lies outside the scope of the present work.

From the n vs. μ curves in Figs. 2 and 3 we computed the numerical derivative of the particle number with respect to the chemical potential to obtain charge compressibility κ. The results for κ^{-1} as a function of the temperature above T_{MIT} (Fig.4) indicate that $\kappa^{-1} \to 0$ as we pass through the MIT.

We also like to mention that in our simulations we observed characteristic effects of enhanced fluctuations and critical slowing down as the MIT is approached. Hence, simulations have to be done with extreme care, appropriately choosing the seeds for the iterative process and gathering many sample points for accurate statistics. In practice we use $\sim 10^5$ MC sweeps and run our calculations in an 8 node parallel cluster. As we approach the critical points, we used up to a few hundred iterations to obtain converged solutions.

We now complement our numerical results with Landau theory arguments. The mean-field equation (2) can be obtained by differentiating the Landau functional [5]

$$F_{\rm LG}[\Delta] = -T \sum_n \frac{\Delta(i\omega_n)^2}{t^2} + F_{\rm imp}[\Delta] \qquad (3)$$

with respect to the hybridization $\Delta(i\omega_n)$ of the SIAM, which has the meaning of a Weiss field. $F_{\rm imp}[\Delta]$ is the free energy of the SIAM in presence of a hybridization. The Green's function of the SIAM is $G(i\omega_n)[\Delta, \alpha] = (1/2T)\delta F_{\rm imp}/\delta\Delta$. This Landau approach was used to describe the Mott transition at half filling [10,11].

As discussed in Ref. [11], the finite temperature Mott transition is a regular bifurcation point. On differentiating the Landau functional twice we get a matrix of the form $-\delta_{nm} + M_{nm}$ where

$$M_{nm} = \frac{t^2}{2T} \left. \frac{\delta^2 F_{\rm imp}[\Delta]}{\delta\Delta(i\omega_n)\delta\Delta(i\omega_m)} \right|_{\rm cp} \qquad (4)$$

acquires a zero mode.

We now make a small change in chemical potential around the critical point and expand the mean field equation(2) to first order in $\delta\alpha = (\mu - \mu_c)$, $\delta\Delta = \Delta(\alpha_c + \delta\alpha) - \Delta(\alpha_c)$. We get,

$$\frac{\delta\Delta(i\omega_n)}{\delta\alpha} = \sum_m \frac{1}{1 - M_{mn}} t^2 \frac{\partial G_{imp}(i\omega_n)}{\partial\alpha} \tag{5}$$

From (2), the lattice occupation at any site which is identical to the local impurity occupation is related to the hybridization by $\langle n\rangle = (2T/t^2)\sum_n \Delta(i\omega_n)$. Thus,

$$\frac{d\langle n\rangle}{d\mu} = 2\sum_n \left[\frac{1}{1 - M}\right] T \frac{\partial G_{imp}(i\omega_n)}{\partial\mu} \tag{6}$$

Clearly, unless the derivative in the *rhs* of (6) is exactly orthogonal to the zero mode of the matrix M, the bifurcation condition leads to the singular behavior of the compressibility. The QMC studies shown above demonstrate that this orthogonality does not occur. The divergence of the compressibility strengthens the liquid-gas picture of the Mott transition presented by Castellani *et. al.* [19].

From the experimental viewpoint, we believe that our results highlight important aspects of the physics of the α-γ transition in Cerium. The detailed description of the non-universal aspects of this material requires more quantitative studies or more elaborate models such as those studied by Held *et. al.* [20]. However, the functional describing these complicated models near the finite temperature Mott transition would reduce to the one underlying the equations we studied. Hence it is plausible that the behavior of the compressibility that we identified in our basic model applies to the α-γ transition of Cerium as well. The divergence of compressibility in the Cerium α-γ transition therefore has an electronic origin and can be understood from model calculations without involving lattice degrees of freedom (which would renormalize values of the critical points without changing qualitative features). In our data, we find a decrease in compressibility during the transition from the insulating to the metallic phase which is similar to what has been measured by Beecroft and Swenson in [21]. According to the results in [21], the compressibility in the low-pressure γ phase (corresponding to the insulating region) is larger than in the high pressure α phase (corresponding to the metallic-like state) at low temperatures, and this effect becomes less noticeable at higher temperatures. Our QMC studies have shown that there is a region of coexistence where the metallic phase is extended into the stability region of the insulating phase, corresponding to the hysteresis observed in the data in [21]. This was also found in X-ray diffraction studies on Cerium [22], where the γ phase was quenched into into the region of stability of the α phase near the phase boundary.

In summary, we presented a careful QMC numerical solution of the doping driven Mott transition in the limit of large lattice connectivity. Our study unveils that the divergence of the compressibility is a generic feature of the confluence of the finite temperature Mott endpoint. We understood this divergence in terms of a simple argument based on Landau theory, which indicates that these results are more general than the specific models for which the numerical studies were carried out. Our results were found to be relevant to the physics of the Cerium α-γ transition.

ACKNOWLEDGMENTS : This research was supported by the Division of Materials Research of the National Science Foundation, under grant NSF DMR 0096462, the Division of Basic Energy Sciences of the Department of Energy under grant US DOE, grant No. DE-FG02-99ER45761. M.J.R. acknowledges support of Fundación Antorchas, CONICET (PID N^o4547/96), and ANPCYT (PMT-PICT1855).

[1] N. F. Mott, *Metal-Insulator Transitions* (Taylor & Francis, 1974).
[2] for a review see M. Imada, A. Fujimori, and Y. Tokura, Rev. Mod. Phys. **70**, 1039 (1998).
[3] B.Johansson, Phil. Mag. **30**, 469 (1974).
[4] for a review see A. Georges, G. Kotliar, W. Krauth, and M. J. Rozenberg, Rev. Mod. Phys. **68**, 13 (1996).
[5] G. Kotliar, Eur. Jour. Phys. B, **11**, 27 (1999).
[6] R. Chitra and G. Kotliar, Phys. Rev. B **63**, 115110 (2001)
[7] W. F .Brinkman and T. M. Rice, Phys. Rev. B, **2**, 4302 (1970)
[8] A.Georges and W.Krauth, Phys. Rev. B, **48**, 7167 (1993).
[9] M. J. Rozenberg, G. Kotliar, and X. Y. Zhang, Phys. Rev. B, **49**, 10181 (1994).
[10] M. J. Rozenberg, R. Chitra, and G. Kotliar. Phys. Rev. Lett., **83**, 3498 (1999).
[11] G. Kotliar, E. Lange and M. J. Rozenberg. Phys. Rev. Lett. **84**, 5180 (2000).
[12] M. J. Rozenberg, G. Kotliar, H. Kajueter, G. A. Thomas, D. H. Rapkine, J. M. Honig, and P. Metcalf, Phys. Rev. Lett., **75**, 105 (1995)
[13] Daniel Fisher, G. Kotliar and G. Moeller. Phys. Rev. B. **52**, 17112 (1995).
[14] N. Furukawa and M. Imada, J. Phys. Soc. Jpn. **60**, 3604 (1991)
[15] M. Kohno Phys. Rev. B **55,** 1435 (1997).
[16] M.C. Gutzwiller, Phys. Rev., **137**, A1726 (1965)
[17] M. J. Rozenberg, Phys. Rev. B, **55**, 4855 (1997)
[18] Jaewook Joo and Viktor Oudovenko, cond-mat/0009367.
[19] C. Castellani, C. Di Castro, D. Feinberg, J. Ranninger Phys. Rev. Lett. **43**, 1957 (1979).
[20] K. Held, A. K. McMahan and R. T. Scalettar, cond-mat/0106599; C. Huscroft, A. K. McMahan and R. T. Scalettar, Phys. Rev. Lett., **82**, 2342 (1999).
[21] R. I. Beecroft and C. A. Swenson, J. Phys. Chem. Solids, **15**, 234(1960).
[22] B. L. Davis and L. H. Adams, J. Phys. Chem. Solids, **25**, 379(1964).